

MULTISCALE FINITE-ELEMENT METHODS FOR ELLIPTIC PROBLEMS IN POROUS MEDIA FLOW

VEGARD KIPPE¹, JØRG E. AARNES¹, AND KNUT-ANDREAS LIE¹

¹SINTEF ICT, Dept. of Applied Mathematics, P.O. Box 124 Blindern, Oslo N-0314, Norway

ABSTRACT

We review two multiscale finite-element methods, the mixed multiscale finite-element method [*Chen and Hou*, 2002; *Aarnes*, 2004] and the numerical subgrid upscaling method [*Arbogast et al.*, 1998; *Arbogast*, 2000, 2002], and demonstrate some of their shortcomings. We then show that combining ideas from both methods yields a new approach that is less likely to suffer from the shortcomings of the original methods. The performance of the new approach is demonstrated by a few numerical experiments.

1. INTRODUCTION

The paper discusses multiscale methods for simulating pressure and fluid velocities in porous media flow. For simplicity, we consider a variable-coefficient Poisson equation describing incompressible, isothermal, one-phase flow

$$\nabla \cdot \mathbf{u} = q, \quad \mathbf{u} = -\mathbf{K}\nabla p, \quad \mathbf{u} \cdot \mathbf{n} = 0 \text{ on } \partial\Omega. \quad (1)$$

One of the major difficulties in simulating flow in porous media is the strong heterogeneity of the medium itself (here reflected in the permeability tensor \mathbf{K}). Porous media are typically heterogeneous at all length scales, which means that the variability increases as the model is refined. Moreover, in applications such as petroleum reservoir simulation, model sizes have long exceeded the capability of existing simulation approaches. The traditional solution to these problems has been to upscale the model using different variations of local averaging, to obtain a model that is both smaller and less heterogeneous. However, the fine-scale heterogeneity may contain particular structures, e.g., channels or fractures, that have a significant impact on the global flow scenario, and these are very hard to account for using any kind of upscaling¹.

Instead of trying to upscale the problem, multiscale methods try to find an approximate solution that contains the most relevant fine-scale information. The result is therefore usually a fine-scale solution. However, the solution is computed from a reduced set of equations on the coarse scale, with the coarse-scale equations being defined in terms of decoupled local problems.

Over the last few years, a number of multiscale methods have been proposed. Here we shall focus on two approaches that are based on the finite-element methodology.

¹To be fair, there exist a few upscaling approaches that aim to incorporate global flow effects. However, these are typically quite expensive since they involve solving a minimization problem (and solving the fine-scale problem once) [*Nielsen and Tveito*, 1998; *Holden and Nielsen*, 2000], or iterating between coarse and fine scales until the upscaled values are consistent in some sense [*Chen et al.*, 2003; *Chen and Durlofsky*].

The first method is the Multiscale Finite-Element Method (MsMFEM) [*Chen and Hou*, 2002; *Aarnes*, 2004], which essentially is based on the idea of generalized basis functions [*Babuska and Osborn*, 1983]. The second method is the Numerical Subgrid Upscaling Method (NSUM) [*Arbogast et al.*, 1998; *Arbogast*, 2000, 2002], which is based on the variational multiscale formulation of *Hughes* [1995]. The ideas underlying the two methods are quite different, and we shall see that by combining these ideas we obtain a new class of potentially more powerful methods.

2. DESCRIPTION OF THE METHODS

Both MsMFEM and NSUM are based on a standard mixed variational formulation of our flow model (1)²: Find $(\mathbf{u}, p) \in H_0^{1,\text{div}}(\Omega) \times L^2(\Omega)$ such that,

$$\begin{aligned} (\mathbf{K}^{-1} \cdot \mathbf{u}, \mathbf{v}) - (p, \nabla \cdot \mathbf{v}) &= 0 & \forall \mathbf{v} \in H_0^{1,\text{div}}(\Omega), \\ (\nabla \cdot \mathbf{u}, l) &= (q, l) & \forall l \in L^2(\Omega). \end{aligned} \quad (2)$$

In the following we shall assume that Ω has been partitioned into a conforming fine polyhedral mesh \mathcal{T}_h , and that a coarse mesh \mathcal{T}_H is formed as a collection of non-overlapping simply connected unions of elements in \mathcal{T}_h . We note that the multiscale methods below can be applied to more general meshes, but these assumptions simplify the presentation.

2.1. The Multiscale Mixed Finite-Element Method. Like any mixed finite-element method for (1), MsMFEM approximates (2) by restricting the solution to lie in finite-dimensional subspaces of $L^2(\Omega)$ and $H_0^{1,\text{div}}(\Omega)$. Naming the MsMFEM approximation spaces for pressure and velocity \mathbf{P}^{ms} and \mathbf{V}^{ms} respectively, we thus seek a solution $(p^{\text{ms}}, \mathbf{u}^{\text{ms}}) \in (\mathbf{P}^{\text{ms}}, \mathbf{V}^{\text{ms}})$ satisfying (2) for all test functions in these discrete spaces.

On the coarse scale, MsMFEM is a generalization of the lowest-order Raviart–Thomas mixed finite-element method (RT0) [*Raviart and Thomas*, 1977]. The MsMFEM approximation space for pressure is equal to the RT0 pressure space of piecewise constants; i.e., $\mathbf{P}^{\text{ms}} = \mathcal{P}_0(\mathcal{T}_H)$. The RT0 velocity space is spanned by basis functions that are piecewise linear in directions normal to element interfaces, meaning that each basis function represents unit flow across one interface. This idea of unit flow across each element interface is kept in MsMFEM, but the basis functions are modified to account for subgrid variation in the coefficients. This may be achieved by letting the basis functions be solutions to local versions of (1), with source terms specified in such a way that unit flow is forced across the element interface. If E_i and E_j denote two coarse elements with a common interface Γ_{ij} , the MsMFEM velocity basis functions $\boldsymbol{\psi}_{ij}$ are defined as follows,

$$\begin{aligned} \boldsymbol{\psi}_{ij} = -\mathbf{K}\nabla\phi_{ij}, \quad \nabla \cdot \boldsymbol{\psi}_{ij} &= \begin{cases} w_i(x)/\int_{E_i} w_i(\xi) \, d\xi, & \text{for } x \in E_i, \\ -w_j(x)/\int_{E_j} w_j(\xi) \, d\xi, & \text{for } x \in E_j, \end{cases} \\ \boldsymbol{\psi}_{ij} \cdot \mathbf{n} &= 0, \quad \text{on } \partial(E_i \cup \Gamma_{ij} \cup E_j). \end{aligned} \quad (3)$$

For certain grids (e.g., tetrahedra and K-orthogonal parallelepipeds), these basis functions reduce to the standard RT0 basis functions if \mathbf{K} and w_i are constant. This definition of the basis functions, first introduced in [*Aarnes and Lie*, 2004], is slightly different from the original definitions in [*Chen and Hou*, 2002] and [*Aarnes*, 2004]. By using (3) and

²See, e.g., [*Brezzi and Fortin*, 1991] for the definition of the function spaces $H_0^{1,\text{div}}(\Omega)$ and $L^2(\Omega)$.

solving simultaneously in both E_i and E_j , the need to specify a boundary condition on Γ_{ij} is eliminated.

In [Aarnes, 2004] it was noted that the MsMFEM solution will be locally mass conservative if the local source term w_i coincides with q in elements containing sources or sinks. For elements where $q = 0$, we may choose w_i arbitrarily, and different approaches have been used. Here we follow [Aarnes et al., 2006] and scale w_i according to the trace of the permeability tensor; i.e., we use

$$w_i(x) = \begin{cases} \text{trace}(\mathbf{K}(x)), & \text{if } q(x)|_{E_i} = 0, \\ q(x), & \text{otherwise.} \end{cases} \quad (4)$$

This completes the definition of the MsMFEM velocity basis functions ψ_{ij} , and the approximation space \mathbf{V}^{ms} is given as $\text{span}\{\psi_{ij}\}$.

2.2. Numerical Subgrid Upscaling. We have seen that MsMFEM essentially is an RT0 method with generalized basis functions on the coarse scale. The numerical subgrid upscaling method was also originally formulated as an RT0 method on the coarse scale [Arbogast et al., 1998], but has proved to be more successful using a higher-order method [Arbogast, 2000, 2002]. Although the formulation is general enough to allow any mixed finite-element method on the coarse scale [Arbogast, 2004], it appears that two particular choices are most popular, namely the first-order Brezzi-Douglas-Marini (BDM1) elements in 2-D [Brezzi et al., 1985], and the first-order Brezzi-Douglas-Duràn-Fortin (BDDF1) elements in 3-D [Brezzi et al., 1987].

Instead of generalizing the coarse-scale basis functions, the NSUM approach is to enrich the approximation spaces by including fine-scale variations, but in a localized way such that fine-scale contributions may be computed independently (of each other and of the coarse-scale solution). Here we shall follow [Arbogast, 2000, 2002] and let the coarse-scale approximation spaces be the BDM1/BDDF1 spaces, with subgrid variations included as subspaces of the fine-grid RT0 space.

Denote by $W_h(E_c)$ the fine-scale RT0 pressure space restricted to coarse element E_c , constrained to have zero average: $W_h(E_c) = \{w_h \in \mathcal{P}_0(\mathcal{T}_h)|_{E_c} : (w_h, 1)_{E_c} = 0\}$. Let $\mathbf{V}_h(E_c)$ be the RT0 velocity space with support strictly inside coarse element E_c ; $\mathbf{V}_h(E_c) = \{\mathbf{v}_h \in \mathbf{V}^{\text{RT0}}(\mathcal{T}_h)|_{E_c} : \mathbf{v}_h \cdot \mathbf{n} = 0 \text{ on } \partial E_c\}$. Finally, let (W_H, \mathbf{V}_H) be the BDM1/BDDF1 approximation spaces over the coarse mesh \mathcal{T}_H . The NSUM approximation spaces are then given as the following direct sums,

$$\begin{aligned} W_{H,h} &= W_H \bigoplus_{E_c \in \mathcal{T}_H(\Omega)} W_h(E_c) = W_H \oplus W_h, \\ \mathbf{V}_{H,h} &= \mathbf{V}_H \bigoplus_{E_c \in \mathcal{T}_H(\Omega)} \mathbf{V}_h(E_c) = \mathbf{V}_H \oplus \mathbf{V}_h. \end{aligned} \quad (5)$$

Each $(\mathbf{u}, p) \in (\mathbf{V}_{H,h}, W_{H,h})$ may be uniquely decomposed into $\mathbf{u} = \mathbf{u}_H + \mathbf{u}_h$ and $p = p_H + p_h$ with $(\mathbf{u}_H, p_H) \in (\mathbf{V}_H, W_H)$ and $(\mathbf{u}_h, p_h) \in (\mathbf{V}_h, W_h)$.

Substituting these representations into (2) yields,

$$\begin{aligned} (\mathbf{K}^{-1} \cdot (\mathbf{u}_H + \mathbf{u}_h), (\mathbf{v}_H + \mathbf{v}_h)) - ((p_H + p_h), \nabla \cdot (\mathbf{v}_H + \mathbf{v}_h)) &= 0, \\ (\nabla \cdot (\mathbf{u}_H + \mathbf{u}_h), (w_H + w_h)) &= (q, (w_H + w_h)), \end{aligned} \quad (6)$$

which should hold for all test functions $(\mathbf{v}_H + \mathbf{v}_h) \in V_{H,h}$ and $(w_H + w_h) \in W_{H,h}$. Using the direct sum decomposition we can now write (6) as separate equations corresponding to the coarse-scale and fine-scale test functions, where the fine-scale equations are localized to each coarse element and therefore decoupled from each other. There is still a coarse/fine coupling, since the fine-scale equations contain the coarse-scale solution \mathbf{u}_H . However, by expressing \mathbf{u}_H as a linear combination of coarse-scale basis functions \mathbf{v}_H , we can compute the fine-scale solution \mathbf{u}_h in terms of the local fine-scale responses to each \mathbf{v}_H , in addition to the response to the source term q . Instead of solving the full set of equations (6), we therefore end up solving multiple fine-scale problems for each coarse element, followed by a single coarse-scale problem. This approach is strongly connected to known techniques in the finite-element literature, such as static condensation, residual-free bubbles, and numerical Green's functions [Hughes, 1995; Brezzi, 1999]. Details for the particular case considered here can be found in [Arbogast, 2002].

2.3. Combining the Two Methods. To be able to independently compute the subgrid contributions, the NSUM method had to localize the fine-scale spaces to each coarse element. This localization may be a severe limitation in cases where the actual flow profile across coarse-element boundaries cannot be represented by the linear profiles of the BDM1/BDDF1 velocity basis functions, e.g., near sources/sinks or high-flow channels. MsMFEM represents inter-element flow in a better way, but is based on a low-order method and will therefore have lower accuracy in smooth regions. Moreover, MsMFEM is more likely to suffer from grid-orientation effects, since the basis functions essentially are designed to capture inter-element flow.

We will now combine the two methods to obtain a scheme that is more general than MsMFEM and allows higher-order methods on the coarse scale, but captures inter-element flow better than NSUM. The crucial point is to remember that the RT0 approximation spaces are contained in the BDM1/BDDF1 spaces. A natural approach therefore seems to be to replace the RT0 part of the NSUM velocity space \mathbf{V}_H by the MsMFEM velocity space \mathbf{V}^{ms} .

More precisely, we search for solutions in $(W_{H,h}, \tilde{\mathbf{V}}_{H,h})$, where $\tilde{\mathbf{V}}_{H,h} = \mathbf{V}_{H,h} - \mathbf{V}^{\text{RT0}} + \mathbf{V}^{\text{ms}}$ and \mathbf{V}^{RT0} denotes the coarse-scale RT0 velocity space. Since the basis functions in \mathbf{V}^{ms} solve equation (1) locally, the fine-scale responses to these basis functions will be zero, as will the response to the fine-scale variation in the source terms. In addition to computing the MsMFEM basis functions, we therefore only need to solve local problems to compute the responses associated with basis functions in BDM1/BDDF1 but not in RT0, and the computational complexity will roughly correspond to the complexity of NSUM.

NSUM is, however, significantly more expensive than MsMFEM. In practice, most of the computational time is spent solving local problems. This means that the ratio of computational times is given approximately as $|\mathbf{V}_H|/|\mathbf{V}^{\text{ms}}| = d$, where d is the number of space dimensions. If we are willing to sacrifice some accuracy, we may obtain a more efficient method by ignoring also the nonzero fine-scale responses. The overall method will then correspond to MsMFEM plus a BDM1/BDDF1 method on the coarse scale, and the computational complexity will be almost the same as for MsMFEM. In the following we shall refer to this latter approach as MsMFEM/BDM1, and write MsMFEM/NSUM when we speak of the approach where all fine-scale contributions are included.

3. NUMERICAL EXPERIMENTS

Next, we compare the performance of the different multiscale methods using three numerical experiments. We restrict ourselves to rectangular elements in 2-D, which means that the NSUM coarse-scale approximation spaces are the BDM1 spaces.

We compute solutions using the multiscale methods with different coarse meshes, and compare the velocity solutions to a reference solution given by the RT0 method applied to the original fine mesh refined four times in each direction. Multiscale methods are often used to obtain fine-scale velocity fields for solving transport equations, and transport solvers typically require fluxes over element edges. We therefore measure how well the multiscale methods reproduce the reference velocity field over the edges of the original fine mesh. Specifically, our error measure is,

$$\epsilon(\mathbf{v}) = \epsilon(\mathbf{v}_x, \mathbf{v}_y) = \|\mathbf{v}_x - \mathcal{I}_{\partial\mathcal{T}_h} \mathbf{v}_x^{\text{ref}}\|_2 + \|\mathbf{v}_y - \mathcal{I}_{\partial\mathcal{T}_h} \mathbf{v}_y^{\text{ref}}\|_2 \quad (7)$$

where $\|\cdot\|_2$ denotes the discrete L^2 -norm computed at element edges and $\mathcal{I}_{\partial\mathcal{T}_h}$ denotes integration over the edges of the original fine mesh.

3.1. Constant Coefficients. Our first experiment is solving the constant-coefficient Poisson equation, i.e., we have $\mathbf{K} = 1$ in (1). The model consists of 64×64 elements, each of size 1×1 , and we use source terms placed in a quarter five-spot pattern, with a unit source in the lower-left corner and a unit sink in the upper-right corner.

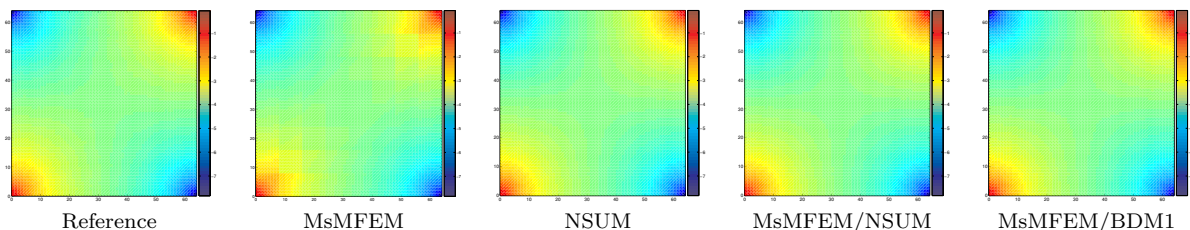


FIGURE 1. Logarithmic plots of the velocity fields for the constant-coefficient model, when using the 8×8 coarse mesh.

TABLE 1. $\epsilon(\mathbf{v})$ for the constant-coefficient model with different coarse meshes.

CDIMS	MsMFEM	NSUM	MsMFEM/NSUM	MsMFEM/BDM1
2×2	0.08686	0.04364	0.04277	0.05564
4×4	0.22895	0.04787	0.04804	0.06268
8×8	0.27050	0.04830	0.04835	0.06016
16×16	0.27258	0.04757	0.04759	0.05114
32×32	0.23429	0.01943	0.01428	0.03057

Figure 1 shows logarithmic plots of the velocity solutions for one of the coarse meshes, and we clearly see some artifacts due to the coarse mesh in the MsMFEM solution. The NSUM solution and the combined methods seem fine in the “picture norm”, which is expected in the constant-coefficient case. From the values of the error measure $\epsilon(\cdot)$ in Table 1, we see that NSUM and MsMFEM/NSUM have almost the same accuracy. This is also expected, since they for this model are equivalent up to the treatment of source

terms. We also note that including the fine-scale contributions corresponding to the extra BDM1 basis functions has little effect on the quality of the solution in this case.

3.2. Diagonal Channel. Next, we consider a model that has proved to be quite challenging for MsMFEM: A single high-permeability channel going diagonally from the source to the sink. Except for the permeability field, the parameters are the same as for the previous model, and Figure 2 shows the velocity fields given by the multiscale methods using the 8×8 coarse mesh. Again we clearly see the influence of the coarse mesh on the MsMFEM solution, but the NSUM solution contains even more artifacts. This clearly illustrates that not allowing fine-scale variations across coarse element edges can be disastrous. There are also some artifacts in the MsMFEM/NSUM and MsMFEM/BDM1 solutions, but the situation is significantly improved compared with the original methods. If we look at the values of $\epsilon(\cdot)$ in Table 2, we see that the errors are quite sensitive to the choice of coarse mesh. However, the relation between the methods remains the same, with MsMFEM/NSUM being the most accurate for (almost) all coarse meshes.

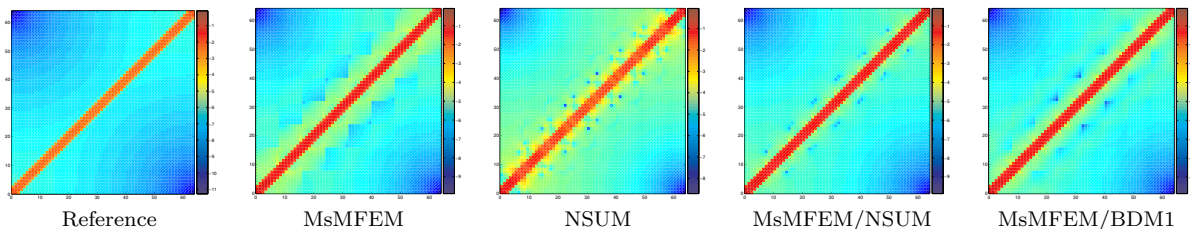


FIGURE 2. Logarithmic plots of the velocity fields for the single-channel model. The coarse mesh has dimensions 8×8 and the permeability ratio is 100.

TABLE 2. $\epsilon(\mathbf{v})$ for the different methods with various coarse-grid sizes.

CDIMS	MsMFEM	NSUM	MsMFEM/NSUM	MsMFEM/BDM1
2×2	1.96392	2.24257	1.33936	1.67350
4×4	1.43002	2.89097	0.84244	1.02826
8×8	0.91713	2.72341	0.27958	0.30353
16×16	0.94423	2.30067	0.30749	0.29631
32×32	1.44821	2.82511	0.91068	1.05699

3.3. Fluvial Reservoir. As our final, and perhaps most realistic example, we shall consider a fluvial reservoir model, where the permeability field contains many narrow high-flow channels. The permeability data are taken from Layer 85 of the 10th SPE Comparison Project [*Christie and Blunt, 2001*], and the fine mesh consists of 60×220 elements. Sources and sinks are placed in a five-spot pattern, with a unit source in the middle and sinks of strength $1/4$ in each of the four corners.

Solutions for a 5×11 coarse mesh are displayed in Figure 3, and they are all quite similar, except for the NSUM solution, which appears to be somewhat smeared out. The complicated channels clearly dominate the flow pattern, and since the main flow direction is normal to the coarse element edges, the MsMFEM basis functions are able to represent

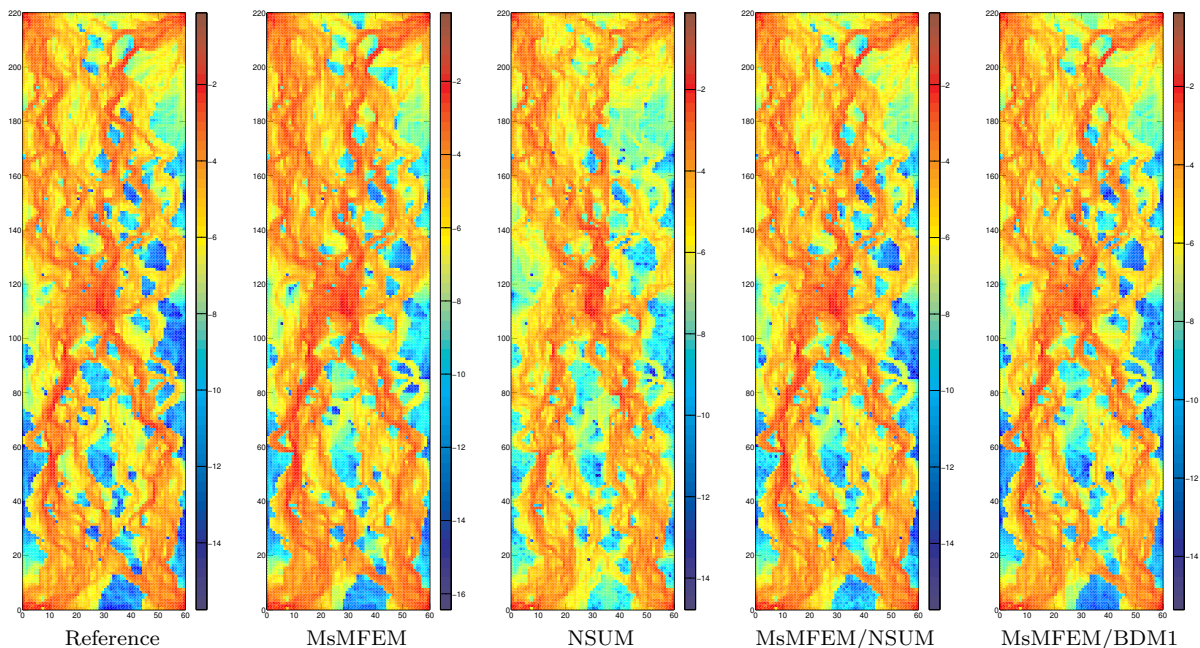


FIGURE 3. Logarithmic plots of the velocity fields for the five-spot pattern on Layer 85 from the 10th SPE Comparison Project [Christie and Blunt, 2001]. The coarse mesh has dimensions 5×11 .

TABLE 3. $\epsilon(\mathbf{v})$ for the different methods with various coarse-grid sizes.

CDIMS	MsMFEM	NSUM	MsMFEM/NSUM	MsMFEM/BDM1
5×11	0.93250	1.78408	0.86237	0.91216
10×22	1.03369	1.79004	0.86539	0.99412
20×55	0.70969	1.88747	0.52560	0.58526
30×110	0.52055	1.51781	0.27949	0.32187

the flow pattern quite well. The effect of increasing the approximation space by the MsMFEM/NSUM or MsMFEM/BDM1 approaches is therefore relatively small in this case, although it depends on the coarse mesh (Table 3).

4. CONCLUDING REMARKS

We have introduced a new multiscale method by combining ideas from MsMFEM and NSUM, and demonstrated that the new method performs better than the original methods on a few simple examples. The new method inherits the possibility of high-order approximation on the coarse scale from NSUM, and is at the same time capable of accurately representing nonlinear velocity profiles across element interfaces because of the MsMFEM basis functions. By choosing to include or neglect local subgrid contributions, one can obtain more efficient or more accurate versions of the method. How to include local subgrid corrections based on adaptivity criteria is a topic for future research.

REFERENCES

- Aarnes, J. E. (2004), On the use of a mixed multiscale finite element method for greater flexibility and increased speed or improved accuracy in reservoir simulation, *SIAM Multiscale Modeling and Simulation*, 2(3), 421–439.
- Aarnes, J. E., and K.-A. Lie (2004), Toward reservoir simulation on geological grid models, in *Proceedings of the 9th European Conference on the Mathematics of Oil Recovery*, EAGE, Cannes, France.
- Aarnes, J. E., S. Krogstad, and K.-A. Lie (2006), A hierarchical multiscale method for two-phase flow based upon mixed finite elements and nonuniform coarse grids, *Multiscale Model. Simul.*, to appear.
- Arbogast, T. (2000), Numerical subgrid upscaling of two-phase flow in porous media, in *Numerical Treatment of Multiphase Flows in Porous Media, Lecture Notes in Physics*, vol. 552, edited by Z. C. et. al., pp. 35–49, Springer, Berlin.
- Arbogast, T. (2002), Implementation of a locally conservative numerical subgrid upscaling scheme for two-phase darcy flow, *Computational Geosciences*, 6(453–481).
- Arbogast, T. (2004), Analysis of a two-scale, locally conservative subgrid upscaling for elliptic problems, *SIAM J. Numer. Anal.*, 42(2), 576–598.
- Arbogast, T., S. E. Minkoff, and P. T. Keenan (1998), An operator-based approach to upscaling the pressure equation, in *Computational Methods in Water Resources XII*, vol. 1, edited by V. N. B. et al., pp. 405–412, Southampton, U.K.
- Babuska, I., and J. Osborn (1983), Generalized finite element methods: their performance and their relation to mixed methods, *SIAM J. Numer. Anal.*, 20, 510–536.
- Brezzi, F. (1999), Interacting with the subgrid world, in *Proceedings of the Conference on Numerical Analysis*, Dundee, Scotland.
- Brezzi, F., and M. Fortin (1991), *Mixed and Hybrid Finite Element Methods*, Computational Mathematics, Springer, New York.
- Brezzi, F., J. D. Jr., and L. D. Marini (1985), Two families of mixed elements for second order elliptic problems, *Numer. Math.*, 47, 217–235.
- Brezzi, F., J. D. Jr., R. Duràn, and M. Fortin (1987), Mixed finite elements for second order elliptic problems in three variables, *Numer. Math.*, 51, 237–250.
- Chen, A., and T. Hou (2002), A mixed multiscale finite element method for elliptic problems with oscillating coefficients, *Mathematics of Computation*, 72(242), 541–576.
- Chen, Y., and L. J. Durlofsky (), Adaptive local-global upscaling for general flow scenarios in heterogeneous formations, submitted to *Transport in Porous Media*.
- Chen, Y., L. J. Durlofsky, M. Gerritsen, and X. H. Wen (2003), A coupled local-global upscaling approach for simulating flow in highly heterogeneous formations, *Advances in Water Resources*, 26, 1041–1060.
- Christie, M. A., and M. J. Blunt (2001), Tenth SPE comparative solution project: A comparison of upscaling techniques, *SPE Reservoir Eval. Eng.*, 4(4), 308–317, url: www.spe.org/csp.
- Holden, L., and B. Nielsen (2000), Global upscaling of permeability in heterogeneous reservoirs; the output least squares (ols) method, *Trans. Porous Media*, 40(2), 115–143.
- Hughes, T. J. R. (1995), Multiscale phenomena: Green’s functions, the dirichlet-to-neumann formulation, subgrid scale models, bubbles and the origins of stabilized methods, *Comput. Methods Appl. Mech. Engrg.*, 127, 387–401.
- Nielsen, B. F., and A. Tveito (1998), An upscaling method for one-phase flow in heterogeneous reservoirs; a Weighted Output Least Squares (WOLS) approach, *Comput. Geosci.*, 2, 92–123.
- Raviart, P. A., and J. M. Thomas (1977), A mixed finite element method for 2nd order elliptic problems, in *Proc. Conf. on Mathematical Aspects of Finite Element Methods, Lecture Notes in Mathematics*, vol. 606, pp. 292–315, Springer, Berlin.